Plant Science 238 (2015) 95–104

Contents lists available at ScienceDirect

Plant Science

journal homepage: www.elsevier.com/locate/plantsci

The control of tomato fruit elongation orchestrated by *sun*, *ovate* and *fs8.1* in a wild relative of tomato

Shan Wu[a], Josh P. Clevenger[a,1], Liang Sun[a], Sofia Visa[b], Yuji Kamiya[c], Yusuke Jikumaru[c], Joshua Blakeslee[a], Esther van der Knaap[a,*]

[a] Department of Horticulture and Crop Science, The Ohio State University, Wooster, OH 44691, USA
[b] Department of Mathematics and Computer Science, The College of Wooster, Wooster, OH 44691, USA
[c] RIKEN Center for Sustainable Resource Science, 1-7-22, Suehiro-cho, Tsurumi-ku, Yokohama 230-0045, Japan

ARTICLE INFO

Article history:
Received 27 April 2015
Received in revised form 24 May 2015
Accepted 28 May 2015
Available online 9 June 2015

Keywords:
Tomato
Near isogenic lines
Fruit shape
SUN
OVATE
fs8.1

ABSTRACT

Within the cultivated tomato germplasm, *sun*, *ovate* and *fs8.1* are the three predominant QTLs controlling fruit elongation. Although *SUN* and *OVATE* have been cloned, their role in plant growth and development are not well understood. To compare and contrast the effects of the three QTLs in a homogeneous background, we developed near isogenic lines (NILs) in the wild species *Solanum pimpinellifolium* LA1589 background. We carried out detailed morphological characterization of reproductive and vegetative organs in the single, double and triple NILs and determined the epistatic interactions of the three loci affecting fruit shape. The phenotypic evaluations demonstrated that the three loci regulate unique aspects of ovary and fruit elongation and in different temporal manners. The strongest effect on organ shape was caused by *sun*. In addition to fruit shape, *sun* also affected leaf and sepal elongation and stem thickness. The synergistic interaction between *sun* and *ovate* or *fs8.1* suggested that the pathways involving *SUN*, *OVATE* and the gene(s) underlying *fs8.1* may converge at a common node. The results of an extensive profiling analysis suggested that the degree of fruit elongation was not related to the accumulation of any of the classical hormones.

1. Introduction

During the domestication and selection of tomato (*Solanum lycopersicum*), a tremendous number of phenotypically distinct cultivars arose. In addition to larger fruit size, which is thought to be the top principle of selection for nearly all fruit-bearing crops, tomato selections also resulted in a large variety of shapes [1]. In contrast to the wild relatives carrying uniformly round fruit, cultivated tomato displays fruit shapes such as flat, round, long and pear-shaped. The elongated shape in particular is a common feature that distinguishes many cultivated varieties from undomesticated accessions. Within the cultivated tomato germplasm pool, elongated shape is predominantly controlled by a combination of the *sun*, *ovate* and *fs8.1* loci [2].

The *sun* and *ovate* loci both have a large effect on fruit elongation, and the underlying genes are known. The *ovate* allele can be found in many obovoid and ellipsoid varieties such as grape tomato. The *sun* allele has a more pronounced effect on shape and is found in very long and tapered shaped heirloom and oxheart tomatoes [1]. *OVATE* was fine-mapped to chromosome 2 and the mutation resulted in a premature stop codon resulting in a null [3]. OVATE is a negative regular of growth, since overexpression of members of the OVATE family proteins (OFPs) leads to dwarf phenotypes in Arabidopsis and tobacco [4,5]. *SUN* encodes a member of the IQD family of calmodulin-binding proteins, and the expression level of the gene is positively associated with elongated shape [6]. The mutation arose from a 24.7-kb duplication event from chromosome 10 to chromosome 7 mediated by the retrotransposon, *Rider* [7]. This event placed *SUN* in a new genome environment leading to higher expression during flower and fruit development [6,8].

The evaluation of a large tomato population led to the hypothesis of the spatiotemporal emergence of the major fruit shape gene mutations during the domestication and selection of cultivated tomato [1]. With respect to the two fruit elongation genes *SUN* and

Abbreviations: ABA, abscisic acid; ANOVA, analysis of variance; CK, cytokinin; GA, gibberellic acid; IAA, indole acetic acid; iP, isopentenyladenine; JA, jasmonic acid; LC–ESI–MS/MS, liquid chromatography–electrospray ionization–tandem mass-spectrometry; NIL, near isogenic line; QTL, quantitative trait locus; SA, salicylic acid; TRA, tryptamine; Trp, tryptophan; WT, wild type.

* Corresponding author. Tel.: +1 330 263 3822; fax: +1 330 263 3887.
E-mail address: vanderknaap.1@osu.edu (E. van der Knaap).
[1] Current address: Institute of Plant Breeding, Genetics, & Genomics, University of Georgia, 1263 Rainwater Rd, Tifton, GA 31793, USA.

http://dx.doi.org/10.1016/j.plantsci.2015.05.019
0168-9452/

OVATE, this model suggests that the *sun* locus emerged relatively recently in Europe after tomato migrated from South and Central America. In contrast, *ovate* is found in Latin American regional and semi-wild *cerasiforme* accessions persisting in populations from Italy and therefore is proposed to be an older mutation.

fs8.1 is another major fruit elongation locus that was first detected in tomato cv. M82 [9], a processing variety classified as "rectangular"-shaped [1]. The mutant allele of *fs8.1* is also found in cv. Howard German and Banana Legs (both also carrying *sun*) and Rio Grande (wild type for *sun* and *ovate*, where *fs8.1* exerts a major impact) [2,10]. Therefore, *fs8.1* may be present in many elongated varieties. The position of the *fs8.1* locus is in the peri-centromeric region of the chromosome, which was inferred by cytological analysis [9]. Its location precludes map-based cloning to identify the underlying gene(s) as a result of reduced recombination in peri-centromeric regions.

Despite the current knowledge, the molecular functions of *SUN*, *OVATE* and the gene(s) underlying *fs8.1* are not well understood. Because the wild type and mutant alleles are not found in the same backgrounds, no empirical comparative study has been conducted to reveal their effects in one background. In this study, we developed a set of near isogenic lines (NILs) of *sun*, *ovate* and *fs8.1* in the wild species *S. pimpinellifolium* LA1589 background by repeated backcrossing and extensive genotyping. The NILs served as a powerful tool for studying detailed effects of each locus, as well as elucidating the genetic interaction among the loci. The evaluation of the reproductive and vegetative phenotypes of the NILs revealed unique features of *sun*, *ovate* and *fs8.1* in regulating organ elongation. The synergistic interactions between *sun* and *ovate*, and *sun* and *fs8.1* suggested that the pathways involving the three genes may converge at a common node in the regulatory network of proximal-distal organ patterning.

2. Materials and methods

2.1. Naming of the loci and the construction of the fruit shape NILs

The naming of the loci is in italicized lowercase letters. The mutant alleles at the three loci are named *sun*, *ovate* and *fs8.1* even though they may not be loss-of-function mutations. For example, *sun* resulted from a gene duplication event and presents a gain-of-function mutation. The introgressions of the three loci are schematically shown in Supplementary Fig. S1. The entire introgressed region at the *sun* locus (86.1 kb on chromosome 7 plus the 24.7-kb insertion) contained 13 annotated genes (ITAG2.4 genomic annotations). Nine were on chromosome 7, and four putative genes including *SUN* (Solyc10g079240) were duplicated from chromosome 10 by the *Rider* transposon-mediated insertion event [6,7]. The *ovate* introgression covered 10 annotated genes including *OVATE*. Because the reference genome of *S. lycopersicum* cv. Heinz 1706 carries the *ovate* mutation, the gene is incorrectly annotated as two, Solyc02g085500 and Solyc02g085510 due to the premature stop codon in the mutant allele. The *fs8.1* introgression region was approximately 50 Mb, and contained a total of 885 annotated genes.

2.2. Plant materials, genotyping and phenotyping

Progeny of a self-pollinated BC_8 plant heterozygous for *sun*, *ovate*, and *fs8.1* were used to select all combinations of the three loci as heterozygous and homozygous. From a total of nearly 800 seedlings, four to five plants of each of the 27 genotypic classes were identified using marker-assisted selection for each of the loci (Supplementary Table S1) and transplanted in the field at the Ohio Agricultural Research and Development Center (OARDC) in Wooster, OH in 2012 in a completely randomized design. Additional plants grown in the greenhouse were used for seed increase and hormone analysis. For floral organ analysis, eight flowers per plant were collected at anthesis. Floral organs were dissected, placed onto an agar plate, and scanned with a table-top scanner at 600 dpi. Measurements were made using ImageJ software (rsbweb.nih.gov/ij/). Anthesis flowers were hand pollinated and tagged in the field. Developing fruit were collected 10 days post anthesis (dpa) and at the ripening stage, cut longitudinally, scanned at 300 dpi, and analyzed for fruit shape using Tomato Analyzer v3.0 [11]. The specific attributes that were measured were shape index, distal end angle, obovoid and proximal eccentricity. Shape index is the ratio of maximum length to width. The distal end angle is measured at the intersection of two lines where the slope is measured via regression along the boundary of the fruit or leaflet on the distal side at a defined distance from the tip of the fruit or leaflet. Obovoid is calculated from the maximum width (W), the height at which the maximum width occurs (y), the average width above that height (w1), the average width below that height (w2), and a scaling function $f(y)$ using the formula: Obovoid = $1/2 \times f(y) \times (1 - w1/W + w2/W)$. Proximal eccentricity is the ratio of the height of the internal ellipse to the distance between the bottom of the ellipse and the top of the fruit (Supplementary Fig. S2; http://www.oardc.ohio-state.edu/vanderknaap/files/Tomato_Analyzer_3.0_Manual.pdf). Leaf phenotypes were evaluated on mature leaves. The measurements of stem thickness, internode length and side branch length were taken at consecutive positions between the 4th and 9th leaves on plants at the 24-leaf stage. The total soluble sugar content (brix) was measured on a puree of five fruits per plant with a handheld refractometer (ATAGO U.S.A., Inc.).

2.3. Statistical analysis

Analysis of variance (ANOVA) and Tukey's mean separation tests were done using the average of the eight flowers, fruits or terminal leaflets as the value for each individual plant. Individual fruit weight was taken as an average of 20 fruits from each plant. Values for each genotype were the average of all plants in a genotype. Analyses of epistasis between two loci using orthogonal contrasts were conducted using all genotypic classes. Contrast coefficients were assigned to each genotype based on the model developed by Cockerham [12] to estimate the type of gene action. For epistatic interaction, the contrast coefficients were multiplied. For example, to calculate the coefficients for additive-by-dominance interaction, the coefficients for additive effect of a locus were multiplied by the coefficients for dominance effect of the other locus. For hierarchical clustering of genotypic classes, values of traits were standardized to have a mean of zero and standard deviation of one across all the genotypes.

2.4. Fruit and terminal leaflet shape modeling and Bayesian classification using contour morphometric data

Unbiased assessment of shape can be accomplished by a morphometric analysis. Two hundred boundary morphometric points (the points were identified along the boundary of the fruit or leaflet at equal distance from one another) were obtained from each longitudinally sliced fruit or leaflet using Tomato Analyzer v3.0 [11]. Elliptic Fourier coefficients were calculated from the morphometric data using 20 harmonics for the fruit shape analysis and 30 harmonics for the terminal leaflets as described previously [13]. The average morphometric points of eight fruits or three leaflets per plant were taken as the representative morphometric points for each individual plant. Clustering of the coefficients for each plant was done using the unsupervised learning Bayesian algorithm of

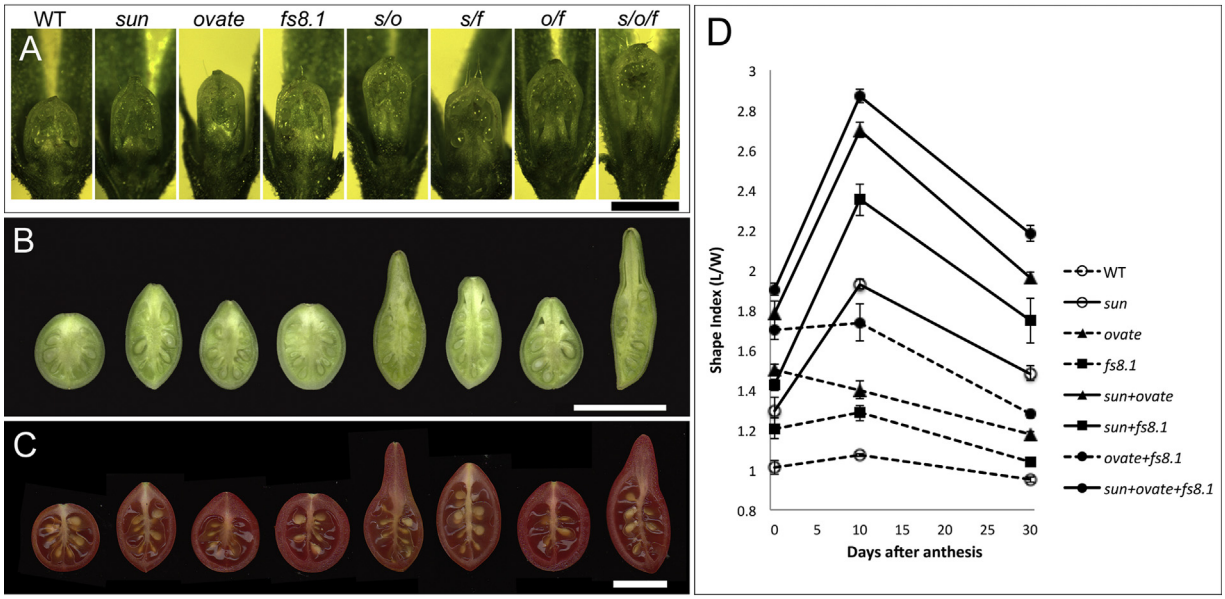

Fig. 1. Ovaries and fruits from the *sun*, *ovate* and *fs8.1* NILs. Representative ovaries and fruits from eight homozygous genotypes are shown in (A–C). (A) Ovaries at anthesis. (B) Fruits at 10 days post anthesis. (C) Ripe fruits. (D) Changes in fruit shape indices from anthesis to fruit maturation of the NILs. Black bar = 1 mm; white bars = 1 cm.

Autoclass [38]. Coefficients of class membership were calculated as the number of plants representing a genotype assigned to one class divided by the total number of plants per genotype.

2.5. Hormone profiling

Hormone profiling was done with tissues collected from field-grown plants that carried the homozygous combinations of the *sun*, *ovate* and *fs8.1*. Only one sample type was used in this analysis, flower buds younger than 9 days before anthesis (dba). The oldest flower bud in the analysis was at a stage when carpels were fused and placenta development was initiated. The reproductive meristems were included in the pooled flower buds. Flower buds were harvested from plants and immediately frozen in liquid nitrogen before being freeze-dried. Flowers from the plants of the same genotype ($n = 4$–5) were pooled into one sample containing about 100–150 mg of fresh weight tissue (from 15 to 20 inflorescences). Tissue collection was repeated four times on different days within 2 weeks between 10 and 11 am. A total of 32 freeze-dried samples (eight genotypes, four replicates) were shipped to RIKEN Plant Science Center, Tsurumi, Yokohama, Japan. Plant hormones were extracted and purified by column cartridge, and analyzed using liquid chromatography–electrospray ionization–tandem mass-spectrometry (LC–ESI–MS/MS) [14]. The hormones analyzed were: Indole-3-acetic acid (IAA), abscisic acid (ABA), cytokinin (CK) in the form of isopentenyladenine (iP), salicylic acid (SA), jasmonic acid (JA) and isoleucine conjugated-JA (JA-Ile). Other measured hormones, namely the CK *trans*-zeatin, the gibberellins (GAs) GA_1 and GA_4, were not included in the statistical analyses due to low levels in the tested tissue and missing data. Brassinosteroids and strigolactones were also not measured. The significance of the effect of a locus on the accumulation of a certain hormone and interactions between loci were calculated by ANOVA. Paired Student's *t*-tests were performed to compare the group means when the effect was significant. The effects of each locus were tested in the WT and mutant backgrounds.

Auxin, tryptophan (Trp) and tryptamine (TRA) levels were analyzed in flower buds younger than 9 dba, anthesis flowers and 5-dpa fruits of different NILs that were immediately frozen in liquid nitrogen. The samples were collected at 10 AM. Approximately 15–20 mg of tissue was weighed and ground in liquid nitrogen and final sample mass was recorded. Samples were extracted with sodium phosphate buffer, pH 7.0 as described previously [15] with the following modifications: samples were extracted at 4 °C, and either 25 ng indole-3-propionic acid (IPA; Santa Cruz Biotech., Dallas, TX, part # sc255215) or a combination of 25 ng deuterated d5-indole-3-acetic acid (Olchemim Ltd., Czech Republic, part # 0311532) and 20 ng deuterated d3-tryptophan (C/D/N Isotopes, Inc., Quebec Canada, part # D-7419) were added as internal standards. Auxin, Trp and TRA were concentrated using solid-phase extraction. Samples were dried under nitrogen gas, re-dissolved in 1 ml methanol, and passed through a 0.2 μm nylon filter (Fisher Scientific, part # 09-720-5). Auxin, Trp and TRA levels were quantified using high-pressure liquid chromatography, tandem mass-spectrometry (Agilent 6460 QQQ LC–MS/MS system) [15]. One microliter of each sample was injected for LC–MS/MS analyses.

3. Results

3.1. The sun, ovate and fs8.1 loci control ovary and fruit elongation before and after anthesis

The phenotypic effects of the each of the three loci were studied using the individual NILs. To evaluate the developmental patterns of fruit elongation regulated by *sun*, *ovate* and *fs8.1* compared to WT, we collected anthesis-stage ovaries and fruits at 10 and 30 dpa from plants carrying homozygous combinations of the three loci. Fruit and ovary elongation can be described by shape index, which is the ratio of maximum height and width. For the single NILs at anthesis, the most elongated ovaries featuring the highest shape index were those carrying *ovate* (Fig. 1A and D; Table 1). *sun* and *fs8.1* also resulted in a higher shape index of the ovary compared to WT (Fig. 1A and D) albeit to a lesser extent than *ovate*. This result suggested that *SUN*, *OVATE* and the gene(s) underlying *fs8.1* contributed to the proximal-distal carpel patterning during floral development before anthesis. The *ovate* mutation resulted in the highest shape index at anthesis, which decreased as the fruit matured (Fig. 1), implying that the *OVATE* gene repressed ovary elongation mainly during floral development. By contrast, the most dramatic effect

Table 1
Comparisons of fruit and leaf shape among NILs.

	Anthesis ovary SI[a]		Ovary length (mm)		Ovary width (mm)		10 dpa fruit SI[a]		Ripe fruit SI[a]	
WT	1.01 ± 0.04	f	1.05 ± 0.02	c	1.04 ± 0.06	ab	1.07 ± 0.01	e	0.95 ± 0.01	g
sun	1.29 ± 0.07	e	1.18 ± 0.04	bc	0.91 ± 0.07	abc	1.93 ± 0.02	c	1.48 ± 0.04	d
ovate	1.50 ± 0.02	cd	1.27 ± 0.03	bc	0.84 ± 0.03	bc	1.40 ± 0.04	d	1.18 ± 0.02	ef
fs8.1	1.21 ± 0.05	ef	1.32 ± 0.11	bc	1.10 ± 0.09	a	1.29 ± 0.02	ed	1.04 ± 0.00	fg
sun/ovate	1.78 ± 0.06	ab	1.47 ± 0.09	abc	0.83 ± 0.03	c	2.70 ± 0.03	a	1.96 ± 0.03	b
sun/fs8.1	1.42 ± 0.09	de	1.40 ± 0.06	abc	0.98 ± 0.05	abc	2.34 ± 0.03	b	1.75 ± 0.11	c
ovate/fs8.1	1.70 ± 0.05	bc	1.68 ± 0.13	ab	0.98 ± 0.04	abc	1.74 ± 0.03	c	1.28 ± 0.02	e
sun/ovate/fs8.1	1.90 ± 0.03	a	1.85 ± 0.02	a	0.97 ± 0.04	abc	2.87 ± 0.03	a	2.21 ± 0.05	a
	Fruit length (mm)		Fruit width (mm)		Fruit distal angle[b]		Obovoid[c]		Proximal eccentricity[c]	
WT	12.48 ± 0.59	d	13.10 ± 0.46	a	134.75 ± 2.62	a	0.067 ± 0.015	c	1.004 ± 0.002	a
sun	17.34 ± 0.36	bc	11.73 ± 0.39	ab	97.06 ± 1.95	cd	0.107 ± 0.020	c	0.936 ± 0.004	ab
ovate	14.05 ± 0.31	d	11.94 ± 0.32	ab	121.70 ± 1.83	ab	0.176 ± 0.008	abc	0.909 ± 0.004	ab
fs8.1	14.58 ± 0.20	cd	14.02 ± 0.18	a	124.05 ± 0.32	ab	0.043 ± 0.013	c	0.987 ± 0.011	a
sun/ovate	20.54 ± 0.45	a	10.51 ± 0.20	b	83.16 ± 1.34	de	0.326 ± 0.013	a	0.666 ± 0.018	c
sun/fs8.1	20.00 ± 0.23	ab	11.63 ± 0.73	ab	84.56 ± 4.58	de	0.120 ± 0.021	bc	0.929 ± 0.008	ab
ovate/fs8.1	15.40 ± 0.53	cd	12.06 ± 0.34	ab	110.70 ± 3.66	bc	0.134 ± 0.030	bc	0.917 ± 0.012	ab
sun/ovate/fs8.1	22.38 ± 0.51	a	10.19 ± 0.35	b	70.82 ± 1.62	e	0.229 ± 0.010	ab	0.762 ± 0.036	bc
	Leaf length (cm)		Terminal leaflet SI[a]		Leaflet length (mm)		Leaflet width (mm)		Leaflet distal angle[b]	
WT	19.6 ± 0.50	b	1.64 ± 0.02	c	52.27 ± 2.27	a	32.10 ± 1.72	abc	43.17 ± 1.67	abc
sun	22.1 ± 0.58	a	1.91 ± 0.02	a	54.49 ± 0.80	a	28.60 ± 0.47	c	34.51 ± 4.57	bcd
ovate	20.7 ± 0.71	ab	1.67 ± 0.03	bc	51.51 ± 2.16	a	30.94 ± 1.31	abc	43.33 ± 1.46	ab
fs8.1	21.4 ± 0.43	ab	1.62 ± 0.02	c	54.06 ± 1.26	a	33.62 ± 1.00	a	47.04 ± 3.83	a
sun/ovate	22.3 ± 0.77	a	1.83 ± 0.03	ab	53.56 ± 1.10	a	29.44 ± 0.67	bc	30.36 ± 2.38	cd
sun/fs8.1	22.2 ± 0.48	a	1.79 ± 0.07	abc	50.55 ± 1.01	a	28.45 ± 0.94	c	30.15 ± 3.95	cd
ovate/fs8.1	20.9 ± 0.57	ab	1.63 ± 0.02	c	53.35 ± 1.78	a	32.88 ± 1.23	ab	42.89 ± 2.12	abc
sun/ovate/fs8.1	22.5 ± 0.67	a	1.74 ± 0.03	bc	51.38 ± 0.87	a	29.64 ± 0.45	abc	28.20 ± 3.20	d

Fruit length, width, distal angle, obvoid and proximal eccentricity were measured on ripe fruits.
Each value represents the mean of four to five plants of the same genotype (eight samples for each plant). Pairwise comparisons between the NILs were done with ANOVA and means were separated with Tukey's test $\alpha < 0.05$.
[a] Shape index (SI) is the $\text{length}_{max} - \text{width}_{max}$ ratio of a fruit, ovary or leaflet.
[b] Distal angles were measured at the position 15% above the distal point of the ripe fruit, and 5% above the tip of the terminal leaflet.
[c] Obovoid and proximal eccentricity describe the pear-shapedness of a fruit.

of *sun* was a large increase in shape index from anthesis to 10 dpa (Fig. 1B and D; Table 1). The shape index then decreased as the fruits matured and width expanded. This proximal-distal patterning resulting from the elevated expression level of *SUN* occurred independent of the other two mutations (Fig. 1D), indicating a strong impact of *SUN* on promoting fruit elongation shortly after fertilization. The *fs8.1* loci by itself caused a slight increase in shape indices of the ovary, 10 dpa and mature fruit, which was not significantly different from WT (Fig. 1; Table 1).

3.2. sun, ovate *and* fs8.1 *affect different aspects of fruit morphology*

To objectively and quantitatively characterize the fruit shapes, mature fruits were analyzed using Tomato Analyzer v3.0 [11]. In addition to shape index, the distal end angle was measured to describe the pointed shape of the fruit. A small angle value implied a pointier fruit. The obovoid attribute described the degree of pear shape and calculated the fraction of the area below and above the midpoint of the fruit. This value increased with more eccentric fruit. The proximal eccentricity value also described the degree of pear shape by calculating the relative position of the seeded area over the total area of the fruit. Thus, a perfectly round fruit would have a large distal end angle, an obovoid value of close to 0 and a proximal eccentricity value of close to 1. Conversely, a pear-shaped fruit would feature a larger obovoid value and a smaller proximal eccentricity value compared to a round fruit. The effect of *sun* on the fruit elongation was evenly distributed along the proximal-distal axis, since the fruit was not visually pear-shaped and the values of obovoid and proximal eccentricity were not significantly different from those of WT (Fig. 1B and C; Table 1). *sun* alone dramatically affected the distal end by resulting in a more pronounced tip that was 30° more acute than WT (Fig. 1B and C; Table 1). *ovate* contributed to a higher shape index by leading to an eccentric positioning of the seeded part (Fig. 1B and C; Table 1), even though the attributes that measured this trait were not always significantly different from WT. Contrary to *sun* and *ovate*, in the wild species background ovary and fruit shape indices of the *fs8.1* single NIL were not significantly different from WT. *sun* and *ovate* increased the length, but decreased the width of the ovary and fruit, hence an increase in shape index (Table 1). However, the ovaries and fruits from *fs8.1* plants were longer, but similar in width if not wider than WT, which could explain why shape index was not significantly different from WT (Table 1). Fruit weight was not significantly different among the single NILs compared to WT (Supplementary Table S2). Yet, *fs8.1* plants tended to have the largest fruit among the single NILs, consistent with the increased length and width of the fruit (Table 1). NILs with *ovate* tended to have smaller fruit (Supplementary Table S2). To evaluate which locus had the greatest effect on fruit elongation, contrasts were performed to compare fruit shape index among different genotypes. The results showed that *sun* had the strongest impact on fruit elongation, whereas *fs8.1* was the least effective among the three loci (Table 2).

3.3. *Interaction of* sun, ovate *and* fs8.1 *on fruit shape*

Visual inspection and mean separation tests suggested that the three loci might interact epistatically (Fig. 1, Table 1). In particular, the combination of *sun* and *ovate* led to an enhanced fruit shape index, as well as the highest obovoid and lowest proximal eccentricity values (Table 1). *sun*, *ovate* and *fs8.1* together led to

Table 2
Comparisons of the effects of *sun*, *ovate* and *fs8.1* on fruit shape index.

	Contrast coefficients											
Comparison	WT	*sun*	*ovate*	*fs8.1*	*s/o*	*s/f*	*o/f*	*s/o/f*	Difference	se	*T*-value	Pr (>|*t*|)
Mutants vs. WT	−7	1	1	1	1	1	1	1	4.23	0.34	12.40	**<0.0001**
sun vs. WT	−1	1	0	0	0	0	0	0	0.53	0.06	8.63	**<0.0001**
ovate vs. WT	−1	0	1	0	0	0	0	0	0.23	0.06	3.68	**0.0009**
fs8.1 vs. WT	−1	0	0	1	0	0	0	0	0.09	0.07	1.26	0.2197
sun vs. *ovate*	0	1	−1	0	0	0	0	0	0.30	0.06	5.25	**<0.0001**
sun vs. *fs8.1*	0	1	0	−1	0	0	0	0	0.44	0.07	6.62	**<0.0001**
ovate vs. *fs8.1*	0	0	1	−1	0	0	0	0	0.14	0.07	2.07	**0.0478**

Table 3
Effects and interactions of *sun*, *ovate* and *fs8.1* on the shape attributes of mature fruits.

	Pr > *F*						
Attribute	*sun*	*ovate*	*fs8.1*	*sun* × *ovate*	*sun* × *fs8.1*	*ovate* × *fs8.1*	*sun* × *ovate* × *fs8.1*
Fruit shape index	**<0.0001**	**<0.0001**	**<0.0001**	**<0.0001**	**0.0150**	0.9576	0.8287
Fruit height	**<0.0001**	**<0.0001**	**<0.0001**	0.0092	0.3274	0.1872	0.9520
Fruit width	**<0.0001**	**<0.0001**	0.7259	0.7711	0.2223	0.3747	0.5921
Distal angle	**<0.0001**	**<0.0001**	**<0.0001**	0.8338	0.6582	0.9876	0.9473
Obovoid	**<0.0001**	**<0.0001**	0.0886	**0.0002**	0.2890	0.2230	0.6631
Proximal eccentricity	**<0.0001**	**<0.0001**	**0.0386**	**<0.0001**	0.0399	**0.0074**	0.1097

Significant effects and interactions were shown by the *p*-values computed from the *F* ratio in ANOVA.

the most elongated anthesis ovary and fruit. Epistasis among the three loci for fruit shape index evaluated by the three-way ANOVA indicated significant interactions of *sun* × *ovate* and *sun* × *fs8.1* (Table 3). Interactions were also observed for *sun* × *ovate* in regulating obovoid and proximal eccentricity, two characteristic traits of pear-shaped fruit (Table 3). These interactions resulted in a more elongated and pear-shaped fruit (Table 1). *fs8.1* did not appear to affect the degree of obovoid (Tables 1 and 3). Although *fs8.1* antagonistically interacted with *ovate* for proximal eccentricity, this value was only slightly larger for *ovate*/*fs8.1* double NIL than that of *ovate* alone (Tables 1 and 3). To determine whether the interactions between loci on fruit shape traits were additive or dominant, orthogonal contrasts were performed for *sun* × *ovate* and *sun* × *fs8.1* on fruit shape index, and for *sun* × *ovate* on obovoid (Supplementary Table S3). All three loci had significant additive effects on fruit shape index, and *sun* interacted with *ovate* and *fs8.1* in an additive-by-additive manner in controlling this trait (Fig. 2; Supplementary Table S3). The effect of *sun* allele was observed in a heterozygous state (Fig. 2), which was consistent with the fact that it is a gain-of-function mutation, and the expression level of *SUN* is positively correlated with organ elongation [6,16]. Given that the premature stop in the OVATE protein could result in a null [3], the mutation was expected to be recessive. However, the *ovate* allele affected fruit elongation in an additive manner (Supplementary Table S3), and the heterozygous *ovate* plants carried more elongated fruit compared to WT (at *ovate*) in the presence of the *sun* allele (Fig. 2), which suggested a dosage effect of *OVATE* or that the mutant allele had partial function. For obovoid, *sun* and *ovate* also interacted in an additive-by-additive manner (Supplementary Table S3). The epistasis between loci demonstrated that combining *sun* with *ovate* or *fs8.1* led to synergistic effect on fruit elongation. Thus, higher expression of *SUN* and the mutation in the *OVATE* gene contributed to enhanced effect on pear-shaped fruit formation.

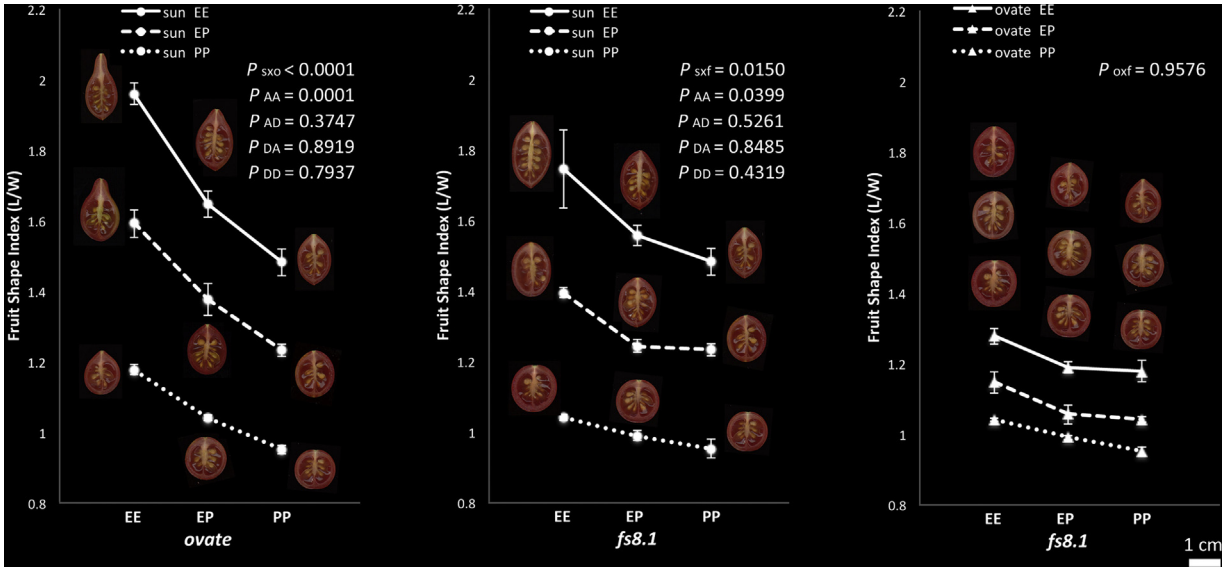

Fig. 2. Epistatic interactions between *sun* and *ovate*, *sun* and *fs8.1* and *ovate* and *fs8.1* on fruit shape index. EE and PP represent the homozygous mutant and WT alleles, respectively, and EP represents the heterozygous state. A and D indicate the additive and dominance effects, respectively. P_{AA}, P_{AD}, P_{DA} and P_{DD} demonstrate the significance of AA, AD, DA and DD interactions between the two loci. Representative fruits of different genotypes are shown.

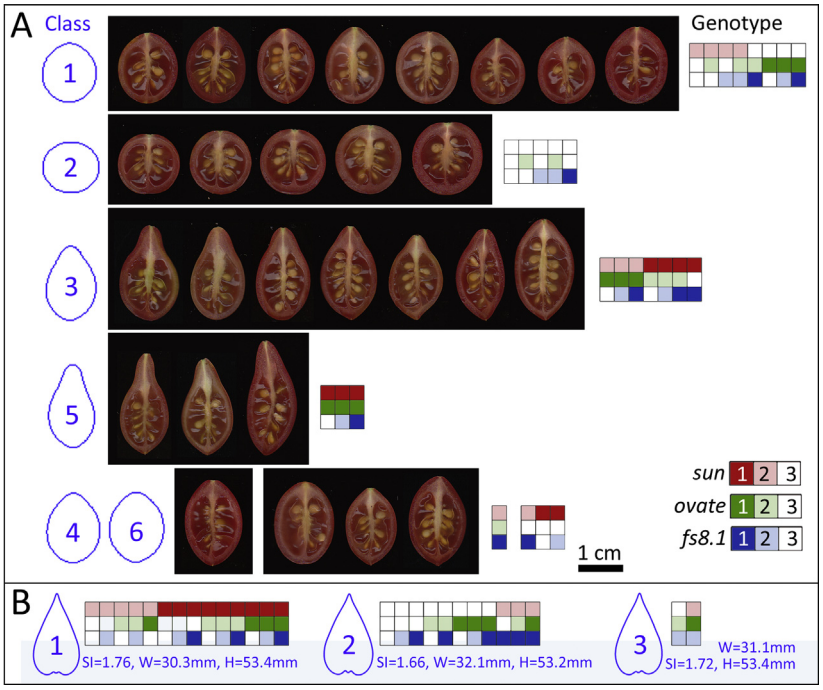

Fig. 3. Shape classification using elliptic Fourier shape modeling and unsupervised learning Bayesian clustering of contour morphometric data. (A) Fruits from plants of all 27 homozygous and heterozygous genotypes of the *sun*, *ovate* and *fs8.1* NILs were classified into six shape categories. Diagrams of the six classes are followed by representative fruits of different genotypes in the same class. The corresponding genotype of each fruit is illustrated by the color panel on the right. The presence of *sun* is indicated by different shades of red; *ovate* is in green and *fs8.1* is in blue. The dark, light shades and blank represent the homozygous mutant (type 1), heterozygous (type 2) and WT (type 3) genotypes, respectively. (B) Terminal leaflets of the 27 genotypes were classified into three shape categories. The genotypic composition of each class is shown by the color panel coded the same way as in (A). Characteristic parameters of each leaflet shape class are shown. SI, shape index; *W*, maximum width; *H*, maximum height.

3.4. *Leaf shape is altered by* sun *but not by* ovate *and* fs8.1

Compelling data support the notion that carpels are modified leaves and that leaves and floral organs are partly interchangeable through modifying only a small set of regulatory genes [17–22]. Several genes known for their roles in tomato fruit growth also have effects on leaf morphology including *SUN* [16,23,24]. However, it is not known whether *ovate* and *fs8.1* play a role in leaf elongation as they do in fruit elongation. To address this question, we compared the leaf phenotypes of the NILs carrying various combinations of the three loci. Consistent with the previous study, *sun* had a dramatic impact on leaves by increasing whole leaf length and terminal leaflet shape index (Table 1). *ovate* and *fs8.1* did not affect the length of the leaf or shape of the terminal leaflet (Table 1; Supplementary Fig. S3). *sun* tended to reduce the distal angle of the terminal leaflet (Table 1; Supplementary Fig. S3B), which was similar to its effect on the distal end feature of the fruit (Table 1; Fig. 1B and C). *ovate* and *fs8.1* did not lead to a more pointed leaflet tip. The *sun*/*ovate*/*fs8.1* triple NIL featured the most pointed leaflets that were significantly different from WT, an effect that appeared to be driven by *sun* (Table 1; Supplementary Fig. S3B). The complexity of the compound leaf measured by the number of primary and intercalary leaflets (Supplementary Table S2, Supplementary Fig. S3A) was not affected by *sun*, *ovate* or *fs8.1* alone or in combination.

3.5. *Modeling of fruit shape and terminal leaflet shape using morphometric data*

The shapes of fruits and leaflets were analyzed above using selected attributes describing the differences among the NILs based on human observation. To further unbiasedly identify different shape classes and reveal the association between the shapes and genotypes, we used contour measurements of scanned fruit and leaflets to perform shape classification analysis using elliptic Fourier shape modeling and Bayesian clustering techniques [13]. Two hundred contour morphometric points were extracted from each fruit with Tomato Analyzer describing the shape in *x*, *y* coordinates. Elliptic Fourier coefficients calculated from the morphometric points were clustered using an unsupervised learning Bayesian algorithm, which identified six distinct fruit shape classes in the data (Fig. 3A). The round (class 2) and pear-shaped (class 5) classes represented the most consistent classes with 100% membership of each genotype assigned to the class (Supplementary Table S4). In the round class (class 2), the fruits were WT or heterozygous for *ovate*, and all were homozygous for the WT allele at *sun* locus. Heterozygosity at the *sun* locus led to elongated shapes in different classes, implying the dominant impact of *sun* on fruit elongation. The pear-shaped class (class 5) described the most elongated and obovoid fruit with high proximal eccentricity. This class was composed of all the genotypes carrying both *sun* and *ovate* in the homozygous state, indicating the synergistic effect of the two mutations in controlling fruit proximal end elongation. *ovate* resulted in different degrees of neck protrusion in classes 1, 3 and 4, and that effect was dependent on *sun*. More specifically, *ovate* in a heterozygous state did not lead to an obvious phenotype on its own as was demonstrated by the fruits in the round class (class 2). However, in the presence of *sun*, the proximal end of the fruits elongated significantly (class 1 and 3). Class 3 described the second most elongated and obovoid fruit. In this class, all the fruits carried *sun* in homozygous or heterozygous state, with combinations of *ovate* and *fs8.1*. Class 1 described slightly elongated fruits with genotypes of either WT or heterozygous for *sun* in various combinations with *ovate* and *fs8.1*. Different combinations of *sun* and *fs8.1* led to evenly elongated fruit in class 6. The use of morphometric points allowed shape measurements to be free of human bias, and represented a true characterization of the inherent shapes. The association between the fruit shape classes and certain combinations of *sun*, *ovate* and *fs8.1* implied additive epistatic interactions,

which supported the gene action and epistatic interaction results shown in Fig. 2 and Supplementary Table S3. Consistent with the finding that *fs8.1* had the least effect on fruit elongation among the three (Table 2), its contribution in driving the shape classification was negligible in the LA1589 background.

Using the same method, the shapes of terminal leaflets were classified into three types (Fig. 3B; Supplementary Table S5) with only subtle differences. Class 1 featured a larger shape index with reduced width compared to class 2, and class 3 was in between class 1 and 2. Due to the asymmetry of the leaflet tip, the distal angle was not well presented by the average morphometric points. Nevertheless, the distribution of genotypes among the shape classes indicated a major impact of *sun* on terminal leaflet elongation, which was consistent with the results of the mean separation tests for leaflet shape index (Fig. 3B; Table 1; Supplementary Fig. S3B).

3.6. *Additional effects of* sun, ovate *and* fs8.1 *on reproductive and vegetative organs development*

The three mutations clearly control elongated fruit shape. To examine whether they also influence the patterning of other floral organs, we measured the length and width of stamens, petals and sepals from anthesis flowers. *sun* had a significant impact on sepal shape (Supplementary Table S2). *fs8.1* also increased the sepal shape index, although the value was not significantly different from WT. *ovate* did not appear to contribute to floral organ shape except for the ovary. Stamens and petals did not exhibit significant differences in shape index in all combinations with the exception of petals of *sun* and *ovate* compared to the *sun*/*ovate*/*fs8.1* triple NIL (Supplementary Table S2).

To explore additional roles of *SUN*, *OVATE* and genes underlying *fs8.1* during vegetative growth, we analyzed plant architectural parameters (Supplementary Table S2). *sun* led to thinner stems, while the other two loci did not have an effect on stem thickness (Supplementary Table S2). Lack of distinguishable differences for internode length and side shoot length (Supplementary Table S2) suggested that neither *sun*, *ovate* nor *fs8.1* had a major impact on plant height and architecture. Flowering time was also similar among the different genotypic classes. We measured brix to determine whether sugar content varied among the NILs and found no association (Supplementary Table S2). This suggested that fruit quality might not have been impacted by the three fruit shape genes.

3.7. *Hormone profiling of the triple NILs developing flowers*

Overexpression of *SUN* leads to parthenocarpic fruits, reminiscent of phenotypes triggered by exogenous auxin or gibberellin (GA) application [6,25]. Moreover, a member of OVATE family protein in Arabidopsis, *AtOFP1*, reduces the expression of *AtGA20ox1* when overexpressed [4,5]. Both auxin and GA regulate critical stages of floral development [26,27]. Other hormones, such as cytokinin (CK) and jasmonic acid (JA) may also participate in floral organ patterning [28–31]. For these reasons we sought to determine the effects of *sun*, *ovate* and *fs8.1* on hormone accumulation. The temporal fruit elongation patterns of *sun*, *ovate* and *fs8.1* compared to WT indicated that ovary elongation was initiated during floral development prior to anthesis. We hypothesized that this effect was early in floral development and therefore measured hormone levels in flower buds younger than 9 days before anthesis (dba) for the hormone profiling. The 9-dba stage corresponded to carpel fusion and placenta initiation stage of ovary development [8]. The ANOVA results showed that *fs8.1* had a pleiotropic effect on the accumulation of different hormones, including IAA, ABA and iP. *sun* significantly affected JA-Ile and *ovate* had an impact on iP accumulation (Table 4). *fs8.1* tended to reduce IAA and increase ABA levels (Fig. 4C). Although the differences were not significant based on the *t*-tests, consistent trends were observed in all backgrounds (Fig. 4C). On the other hand, the effect of *fs8.1* on iP was dependent on the genotypes at the *ovate* locus (Fig. 4C). *ovate* and *fs8.1* significantly interacted in affecting the accumulation of iP and had opposite effects (Table 4; Fig. 4B and C). *ovate* reduced the iP levels in the *fs8.1* mutant background, whereas *fs8.1* increased iP levels in the absence of the *ovate* mutation (Fig. 4B and C). An interaction was also found between *ovate* and *fs8.1* for SA (Table 4). *ovate* significantly reduced SA levels only in the *fs8.1* WT background (Fig. 4B). The interaction between *fs8.1* and *sun* was significant for JA and JA-Ile (Table 4). *sun* increased JA and JA-Ile levels in the absence of the *fs8.1* mutation (Fig. 4A), whereas the positive effect of *fs8.1* on JA and JA-Ile accumulation was only seen in the *sun* WT background (Fig. 4C). Even though the differences were marginal in the youngest floral stages, we sought to explore further the impact of the three loci on the accumulations of auxin and its precursors, tryptophan (Trp) and tryptamine (TRA), at other stages of floral and fruit development. Unlike the prior experiment, *fs8.1* did not have a significant effect on IAA accumulation in the young flower buds (Supplementary Fig. S4B). The only significant finding was that *fs8.1* reduced TRA accumulation in 5-dpa fruits in all backgrounds (Table 4; Fig. 4D).

4. Discussion

4.1. *SUN, OVATE and fs8.1 appear to function in different but related pathways*

In cultivated tomato, various alleles contribute to fruit shape and size differences among the many accessions [1,32,33]. Accurate comparisons of the effect of several fruit morphology loci have not been possible until the development of NILs in a homogeneous background. For this study, we purposely developed NILs containing one or combinations of the three elongation loci. This resource finally allowed a detailed comparison of the main phenotypic effects of each fruit elongation locus by itself and in combination. Moreover, NILs allowed us to evaluate epistatic relationships without the influence from other segregating fruit shape and size loci. Our results indicated that each of the three loci contributed to organ elongation in a distinct way. From the temporal perspective, *sun* resulted in a more elongated ovary before and more significantly after anthesis, consistent with what has been reported previously [8,16]. On the other hand, *ovate* affected ovary elongation entirely prior to anthesis. The shape index decreased from anthesis to 10 dpa till maturation, which is likely the result of a process that is not actively controlled by *ovate*. *fs8.1* contributed to ovary elongation at anthesis in the LA1589 background. Although the effect was not significant, the trend was consistent with a previous study carried out in the cultivated tomato M82 background, showing that *fs8.1* also sets the elongated pattern before anthesis [34]. These findings suggest that *OVATE* and the gene(s) underlying *fs8.1* act mainly during floral development, while *SUN* exerts its main effect during the period of intensive cell division after fertilization. LA1589 has a highly predictable inflorescence growth pattern [8,35]. Therefore, the LA1589 NILs will be a useful resource in future studies of the fruit-shape gene activities during floral development. Once it is known when the effects of the genes become visible, the specific development circumstance and context of the regulatory network during that stage will provide crucial insights into the function of the fruit shape genes. In addition to the temporal manner, the differences among the three loci were also demonstrated by the unique features of the elongated fruits. Compared to *sun*, which resulted in evenly elongated fruit, *ovate* led to elongation at the proximal end. Unlike *sun*, which elongates the fruit by

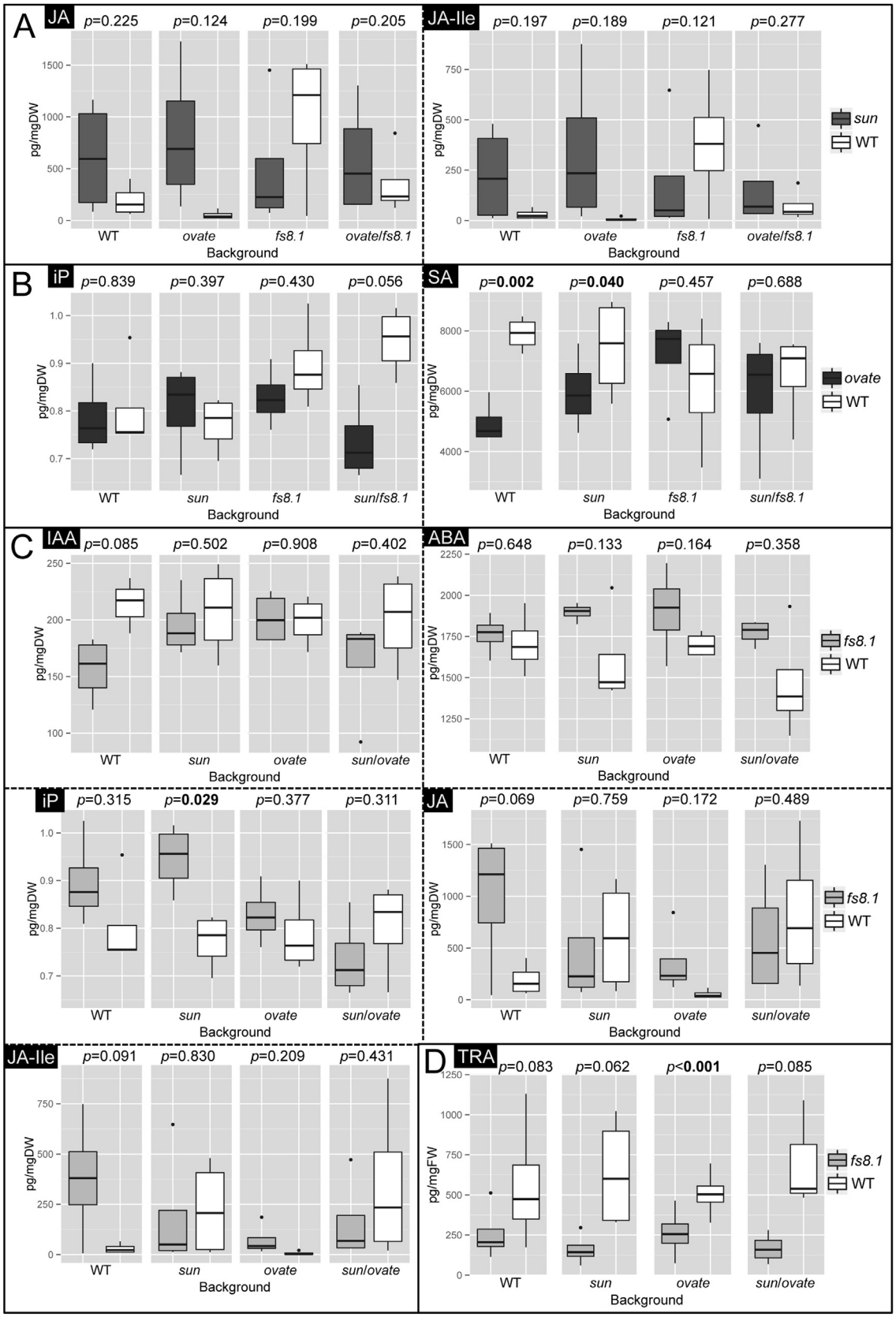

Fig. 4. Effects of *sun*, *ovate* and *fs8.1* on hormone accumulation. Except for trypatamine (TRA), which was measured in 5-dpa fruits from greenhouse-grown plants, all the other data were from pooled flower buds younger than 9 dba collected on field-grown plants. For each locus, the hormone levels of the mutant were compared to those of WT in different backgrounds, and the *p*-values of paired *t*-tests are shown. (A) *sun* increased JA and JA-Ile levels in the absence of *fs8.1* mutation. (B) *ovate* reduced the iP levels in *fs8.1* mutant background and reduced the SA levels in the absence of *fs8.1* mutation. (C) *fs8.1* reduced the levels of IAA, and increased the levels of ABA. *fs8.1* also increased the levels of iP, JA and JA-Ile dependent on the genotypes at *ovate* and *sun* loci. (D) *fs8.1* reduced the TRA accumulation in 5-dpa fruits. pg/mg DW, pg per mg dry weight; pg/mg FW, pg/mg frozen weight of fresh tissue.

Table 4
Effects and interactions of *sun*, *ovate* and *fs8.1* on hormone levels.

	Prob > *F*						
Hormone	*sun*	*ovate*	*fs8.1*	*sun* × *ovate*	*sun* × *fs8.1*	*ovate* × *fs8.1*	*sun* × *ovate* × *fs8.1*
IAA	0.7395	0.6603	**0.0237**	0.2026	0.7632	0.3626	0.0539
ABA	0.2519	0.6514	**0.0063**	0.1800	0.2406	0.5685	0.6483
iP	0.6267	**0.0324**	**0.0495**	0.4311	0.8161	**0.0190**	0.1124
SA	0.8458	0.0685	0.8857	0.9849	0.4724	**0.0338**	0.1650
JA[a]	0.0672	0.4765	0.1416	0.1003	**0.0245**	0.7347	0.7441
JA-Ile[a]	**0.0410**	0.3158	0.1099	0.0781	**0.0173**	0.8636	0.7153
Tryptamine_5dpa	0.9985	0.8683	**0.0002**	0.7772	0.2050	0.9939	0.7429

Expect for tryptamine, which was measured on 5-dpa fruits from greenhouse-grown plants, all the other hormone data were generated using young flower buds of field-grown plants.
Significant effects and interactions were shown by *p*-values computed from the *F* ratio in ANOVA.
[a] Log transformed data were used for ANOVA of JA and JA-Ile.

redistributing the mass, *fs8.1* appeared to promote the growth along the proximal-distal axis while not reducing fruit width, which led to a larger fruit albeit not significantly (Supplementary Table S2). These results imply that *SUN*, *OVATE* and the gene(s) underlying *fs8.1* may function via different pathways during various spatial and temporal windows in ovary and fruit development.

While it appears that the shape loci act in different pathways, synergistic interactions between *sun* and *ovate*, and *sun* and *fs8.1* suggested that the pathways involving these fruit shape genes may instead converge at certain nodes, and that one mutation enhanced the effects of the other mutation. The *ovate* allele in the LA1589 background did not lead to a typical pear-shaped fruit with highly pronounced proximal protrusion as is found in the Yellow Pear variety [3]. Results from this study showed that *sun* enhanced the effect of the *ovate* in controlling the pear-shaped fruit form. However, whereas *sun* × *ovate* resulted in pear-shaped fruit, the effect of *ovate* is also enhanced into a distinct pear-shaped form by two unrelated suppressor loci, *sov1* and *sov2* [36]. Further, comparisons among the LA1589 NILs showed that *fs8.1* alone did not significantly affect the elongation and size of the fruit. However, *fs8.1* dramatically increases fruit shape index and fruit weight in the cultivated tomato M82 background [34]. These results suggest that the effect of *SUN*, *OVATE* and the gene(s) underlying *fs8.1* is dependent on the genetic background and controlled by several other genes in controlling fruit elongation.

4.2. *The overall morphological influence of* sun, ovate *and* fs8.1

Among the three fruit shape loci, *ovate* seemed to only impact ovary elongation, while *sun* regulated the growth of multiple floral organs and vegetative parts including the leaf and stem. *fs8.1* had the least effect on fruit elongation. To gain an overall picture of how the three loci individually and collectively impact the reproductive and vegetative phenotypes, the eight homozygous genotypes were hierarchically clustered using all significantly different traits among the NILs (Fig. 5). Distinctly different from WT, all the genotypes carrying *sun* were clustered together, featuring a dramatic increase in the length of both reproductive and vegetative organs, a reduction in organ width (including a thinner stem), and the distal angles of fruit and leaflet. Similar to how *sun* influences the temporal pattern of fruit elongation (Fig. 1D), the phenotypes associated with this locus were observed regardless of the presence of *ovate* and *fs8.1*, which suggests a more prominent effect of *SUN* on plant growth compared to the other two genes. Plants carrying only *fs8.1* behaved most similar to WT, except for longer leaves and more elongated sepals. *ovate* alone led to a few differences compared to WT, including higher shape index of the anthesis ovary resulted from reduced width and increased length, and lower proximal eccentricity and higher obovoid values of the fruit. *ovate* and *fs8.1* combined led to a more elongated ovary at anthesis, while the remainder of the traits was similar to the *ovate* single NIL. In contrast to the limited overall influence of *fs8.1* and *ovate*, the dramatic impact of *sun* on both reproductive and vegetative growth suggested a broader role of the *SUN* gene in regulating plant growth.

4.3. *Hormone accumulation is not greatly impacted by* sun, ovate *and/or* fs8.1

Previous studies on SUN and the OVATE family proteins hypothesized possible links to the auxin and GA pathways [5,16]. However, the hormone profiling analysis using young flower buds of the *sun*, *ovate*, *fs8.1* NILs did not show association between *sun* or *ovate* and auxin or GA level. *sun* and *ovate*, which together resulted in pear-shaped fruit formation, led to changes in different sets of

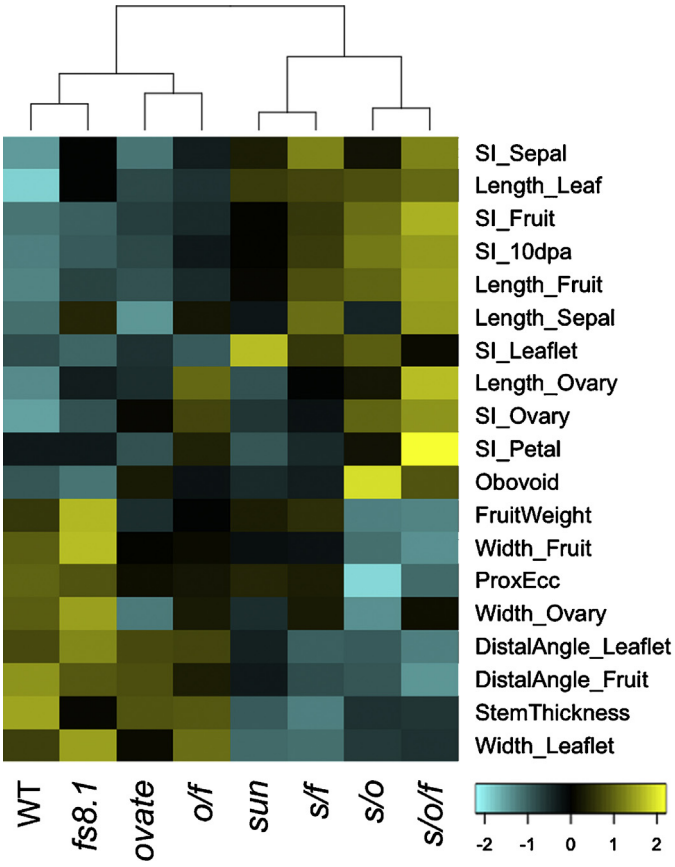

Fig. 5. Hierarchical clustering of eight homozygous genotypes of the NILs with traits measured in this study. Values of traits were standardized to have a mean of zero and standard deviation of one across all the genotypes. SI, shape index; ProxEcc, proximal eccentricity; Fruit, ripe fruit; 10 dpa, 10-dpa fruit; Leaflet, terminal leaflet.

hormones, suggesting that the synergistic effect on fruit morphology resulted from the interaction between *sun* and *ovate* was not mediated through a common hormone pathway. Although the plants singly carrying *sun* and *fs8.1* both had elevated JA and JA-Ile levels, the *sun*/*fs8.1* double mutant that exhibited more elongated shapes did not accumulate more JA or JA-Ile than the single mutants. *fs8.1* had the broadest impact on different hormones, which may be the result of the combined activity of the 19 hormone-metabolism-related genes (functionally annotated using MapMan, [37]) among the 885 genes in the *fs8.1* introgression. A small sample size of four replicates was employed in this study, which limited the interpretation of the data. Nevertheless, there was no clear positive or negative correlation between the levels of a tested hormone and the degrees of ovary or fruit elongation resulted from different combination of the three loci, which suggested the promotion of fruit elongation by *sun*, *ovate* and *fs8.1* was not a direct result of their effects on the accumulation of these hormones.

Acknowledgments

This work was supported by National Science Foundation IOS 0922661. We thank Drs. J.C. Jang, M.L. Jones, R.S. Lamb and E.J. Stockinger for helpful comments.

Appendix A. Supplementary data

Supplementary data associated with this article can be found, in the online version, at http://dx.doi.org/10.1016/j.plantsci.2015.05.019

References

[1] G.R. Rodriguez, S. Munos, C. Anderson, S.C. Sim, A. Michel, M. Causse, B.B. McSpadden Gardener, D. Francis, E. van der Knaap, Distribution of SUN, OVATE, LC, and FAS in the tomato germplasm and the relationship to fruit shape diversity, Plant Physiol. 156 (2011) 275–285.
[2] M.J. Gonzalo, E. van der Knaap, A comparative analysis into the genetic bases of morphology in tomato varieties exhibiting elongated fruit shape, Theor. Appl. Genet. 116 (2008) 647–656.
[3] J. Liu, J. Van Eck, B. Cong, S.D. Tanksley, A new class of regulatory genes underlying the cause of pear-shaped tomato fruit, Proc. Natl. Acad. Sci. U.S.A. 99 (2002) 13302–13306.
[4] J. Hackbusch, K. Richter, J. Muller, F. Salamini, J.F. Uhrig, A central role of *Arabidopsis thaliana* ovate family proteins in networking and subcellular localization of 3-aa loop extension homeodomain proteins, Proc. Natl. Acad. Sci. U.S.A. 102 (2005) 4908–4912.
[5] S. Wang, Y. Chang, J. Guo, J.G. Chen, Arabidopsis Ovate Family Protein 1 is a transcriptional repressor that suppresses cell elongation, Plant J. 50 (2007) 858–872.
[6] H. Xiao, N. Jiang, E.K. Schaffner, E.J. Stockinger, E. Van der Knaap, A retrotransposon-mediated gene duplication underlies morphological variation of tomato fruit, Science 319 (2008) 1527–1530.
[7] N. Jiang, D. Gao, H. Xiao, E. van der Knaap, Genome organization of the tomato sun locus and characterization of the unusual retrotransposon Rider, Plant J. 60 (2009) 181–193.
[8] H. Xiao, C. Radovich, N. Welty, J. Hsu, D. Li, T. Meulia, E. van der Knaap, Integration of tomato reproductive developmental landmarks and expression profiles, and the effect of SUN on fruit shape, BMC Plant Biol. 9 (2009) 49.
[9] S. Grandillo, H.-M. Ku, S.D. Tanksley, Characterization of fs8 1, a major QTL influencing fruit shape in tomato, Mol. Breed. 2 (1996) 251–260.
[10] M.T. Brewer, L. Lang, K. Fujimura, N. Dujmovic, S. Gray, E. van der Knaap, Development of a controlled vocabulary and software application to analyze fruit shape variation in tomato and other plant species, Plant Physiol. 141 (2006) 15–25.
[11] G.R. Rodriguez, J.B. Moyseenko, M.D. Robbins, N.H. Morejon, D.M. Francis, E. van der Knaap, Tomato analyzer: a useful software application to collect accurate and detailed morphological and colorimetric data from two-dimensional objects, J. Vis. Exp. 16 (2010) 37.
[12] C.C. Cockerham, An extension of the concept of partitioning hereditary variance for analysis of covariances among relatives when epistasis is present, Genetics 39 (1954) 859–882.
[13] S. Visa, C.X. Cao, B.M. Gardener, E. van der Knaap, Modeling of tomato fruits into nine shape categories using elliptic fourier shape modeling and Bayesian classification of contour morphometric data, Euphytica 200 (2014) 429–439.
[14] M. Seo, Y. Jikumaru, Y. Kamiya, Profiling of hormones and related metabolites in seed dormancy and germination studies, Methods Mol. Biol. 773 (2011) 99–111.
[15] O. Novak, E. Henykova, I. Sairanen, M. Kowalczyk, T. Pospisil, K. Ljung, Tissue-specific profiling of the *Arabidopsis thaliana* auxin metabolome, Plant J. 72 (2012) 523–536.
[16] S. Wu, H. Xiao, A. Cabrera, T. Meulia, E. van der Knaap, SUN regulates vegetative and reproductive organ shape by changing cell division patterns, Plant Physiol. 157 (2011) 1175–1186.
[17] E. Coen, Goethe and the ABC model of flower development, C. R. Acad. Sci. III 324 (2001) 523–530.
[18] J.W. Goethe, Italian Journey, Penguin Classics, London, 1970.
[19] T. Honma, K. Goto, Complexes of MADS-box proteins are sufficient to convert leaves into floral organs, Nature 409 (2001) 525–529.
[20] H. Alonso-Cantabrana, J.J. Ripoll, I. Ochando, A. Vera, C. Ferrandiz, A. Martinez-Laborda, Common regulatory networks in leaf and fruit patterning revealed by mutations in the Arabidopsis ASYMMETRIC LEAVES1 gene, Development 134 (2007) 2663–2671.
[21] L. Ostergaard, Don't 'leaf' now, the making of a fruit, Curr. Opin. Plant Biol. 12 (2009) 36–41.
[22] S. Pelaz, R. Tapia-Lopez, E.R. Alvarez-Buylla, M.F. Yanofsky, Conversion of leaves into petals in Arabidopsis, Curr. Biol. 11 (2001) 182–184.
[23] B. Molesini, T. Pandolfini, G.L. Rotino, V. Dani, A. Spena, Aucsia gene silencing causes parthenocarpic fruit development in tomato, Plant Physiol. 149 (2009) 534–548.
[24] H. Wang, B. Jones, Z. Li, P. Frasse, C. Delalande, F. Regad, S. Chaabouni, A. Latche, J.C. Pech, M. Bouzayen, The tomato Aux/IAA transcription factor IAA9 is involved in fruit development and leaf morphogenesis, Plant Cell 17 (2005) 2676–2692.
[25] M. de Jong, M. Wolters-Arts, R. Feron, C. Mariani, W.H. Vriezen, The *Solanum lycopersicum* auxin response factor 7 (SlARF7) regulates auxin signaling during tomato fruit set and development, Plant J. 57 (2009) 160–170.
[26] H. Yu, T. Ito, Y. Zhao, J. Peng, P. Kumar, E.M. Meyerowitz, Floral homeotic genes are targets of gibberellin signaling in flower development, Proc. Natl. Acad. Sci. U.S.A. 101 (2004) 7827–7832.
[27] Y. Cheng, X. Dai, Y. Zhao, Auxin synthesized by the YUCCA flavin monooxygenases is essential for embryogenesis and leaf formation in Arabidopsis, Plant Cell 19 (2007) 2430–2439.
[28] T. Ito, K.H. Ng, T.S. Lim, H. Yu, E.M. Meyerowitz, The homeotic protein AGAMOUS controls late stamen development by regulating a jasmonate biosynthetic gene in Arabidopsis, Plant Cell 19 (2007) 3516–3529.
[29] I. Bartrina, E. Otto, M. Strnad, T. Werner, T. Schmulling, Cytokinin regulates the activity of reproductive meristems, flower organ size, ovule formation, and thus seed yield in *Arabidopsis thaliana*, Plant Cell 23 (2011) 69–80.
[30] F. Brioudes, C. Joly, J. Szecsi, E. Varaud, J. Leroux, F. Bellvert, C. Bertrand, M. Bendahmane, Jasmonate controls late development stages of petal growth in *Arabidopsis thaliana*, Plant J. 60 (2009) 1070–1080.
[31] N. Marsch-Martinez, D. Ramos-Cruz, J. Irepan Reyes-Olalde, P. Lozano-Sotomayor, V.M. Zuniga-Mayo, S. de Folter, The role of cytokinin during *Arabidopsis gynoecia* and fruit morphogenesis and patterning, Plant J. 72 (2012) 222–234.
[32] I. Paran, E. van der Knaap, Genetic and molecular regulation of fruit and plant domestication traits in tomato and pepper, J. Exp. Bot. 58 (2007) 3841–3852.
[33] S.D. Tanksley, The genetic, developmental, and molecular bases of fruit size and shape variation in tomato, Plant Cell 16 (Suppl.) (2004) S181–S189.
[34] H.M. Ku, S. Grandillo, S.D. Tanksley, fs8.1, a major QTL, sets the pattern of tomato carpel shape well before anthesis, Theor. Appl. Genet. 101 (2000) 873–878.
[35] N. Welty, C. Radovich, T. Meulia, E. van der Knaap, Inflorescence development in two tomato species, Can. J. Bot. 85 (2007) 111–118.
[36] G.R. Rodriguez, H.J. Kim, E. van der Knaap, Mapping of two suppressors of OVATE (sov) loci in tomato, Heredity 111 (2013) 256–264.
[37] B. Usadel, A. Nagel, O. Thimm, H. Redestig, O.E. Blaesing, N. Palacios-Rojas, J. Selbig, J. Hannemann, M.C. Piques, D. Steinhauser, W.R. Scheible, Y. Gibon, R. Morcuende, D. Weicht, S. Meyer, M. Stitt, Extension of the visualization tool MapMan to allow statistical analysis of arrays, display of corresponding genes, and comparison with known responses, Plant Physiol. 138 (2005) 1195–1204.
[38] F. Achcar, J.-M. Camadro, D. Mestivier, AutoClass@IJM: a powerful tool for Bayesian classification of heterogeneous data in biology, Nucleic Acids Res. 37 (2009) W63–W67.